A Common Structural Motif in the Binding of Virulence Factors to Bacterial Secretion Chaperones

Mirjana Lilic,[1] Milos Vujanac,[1] and C. Erec Stebbins[1,*]
[1] Laboratory of Structural Microbiology
The Rockefeller University
New York, New York 10021

Summary

Salmonella invasion protein A (SipA) is translocated into host cells by a type III secretion system (T3SS) and comprises two regions: one domain binds its cognate type III secretion chaperone, InvB, in the bacterium to facilitate translocation, while a second domain functions in the host cell, contributing to bacterial uptake by polymerizing actin. We present here the crystal structures of the SipA chaperone binding domain (CBD) alone and in complex with InvB. The SipA CBD is found to consist of a nonglobular polypeptide as well as a large globular domain, both of which are necessary for binding to InvB. We also identify a structural motif that may direct virulence factors to their cognate chaperones in a diverse range of pathogenic bacteria. Disruption of this structural motif leads to a destabilization of several chaperone-substrate complexes from different species, as well as an impairment of secretion in *Salmonella*.

Introduction

Type III secretion systems (T3SS) are central to the virulence of a wide variety of animal and plant pathogens and commensals, including such human scourges as typhoid fever, the plague, and bacillary dysentery (Galan and Collmer, 1999). T3SS are used to translocate bacterial proteins into host cells (Cornelis, 2000; Galan, 2001; Galan and Collmer, 1999; Hueck, 1998; Zaharik et al., 2002). The virulence factor substrates of T3SS are biochemically diverse, manipulating host cell biological systems such as cytoskeletal structure, signal transduction, cell cycle progression, and programmed cell death, allowing bacteria to precisely modulate host tissues and systems for the benefit of the pathogen (Barbieri et al., 2002; Lerm et al., 2000; Schiavo and van der Goot, 2001; Stebbins and Galan, 2001b).

The pathogenic T3SS substrates are multidomain proteins that are typically subdivided into two distinct regions: an N-terminal domain that contains secretion and translocation signals that function within the bacterium, and one or more C-terminal domains that harbor the host cell effector activities (Ghosh, 2004; Parsot et al., 2003). The first 15–20 amino acids are known to be required for secretion, although controversy exists concerning their nature as a peptide and/or mRNA signal (Ghosh, 2004; Ramamurthi and Schneewind, 2003). Following the secretion signal is a small 50–100 amino acid domain that is responsible for binding secretion chaperones in the bacterium and targeting the virulence factors

to the pathogenic secretion system (Lee and Galan, 2004).

Biochemically, the T3SS chaperones are small acidic proteins, show no ATP binding or hydrolytic activity, possess no easily detectable sequence similarity to other proteins or other T3SS chaperones, and form highly stable dimers in solution (Ghosh, 2004; Parsot et al., 2003; Stebbins and Galan, 2003; Wattiau et al., 1996). Cocrystal structures of chaperone-virulence factor complexes have revealed that the N-terminal chaperone binding domains (CBD) interact with their chaperones in a highly unusual manner, forming extended, nonglobular polypeptides that wrap around both chaperones in the dimer through interactions with large hydrophobic patches (Birtalan et al., 2002; Phan et al., 2004; Schubot et al., 2005; Stebbins and Galan, 2001a). These cocrystal structures and the structures of several T3SS chaperones alone have shown that, despite the lack of detectable sequence identity, the chaperones comprise a related family of molecules, sharing similar folds and surface hydrophobic elements for binding to their substrates (Luo et al., 2001; Phan et al., 2004; Singer et al., 2004; van Eerde et al., 2004).

Gram-negative bacteria possessing T3SS express thousands of proteins, and yet only a handful are secreted through these systems. Despite the high degree of structural and functional conservation in the chaperones, there has been little progress toward synthesizing a unified view of how these substrates are targeted to their chaperones or to the pathogenic T3SS. In particular, no common amino acid motifs have been identified to play such roles, although, in the context of the chaperone-CBD complexes, generalized similarities in the hydrophobic interactions between chaperones and their substrates have been discussed (Ghosh, 2004; Stebbins and Galan, 2003).

Although most T3SS chaperones bind a single substrate, InvB of *Salmonella* and Spa15 of *Shigella* are dramatic exceptions (Parsot et al., 2003). InvB binds to at least four invasion proteins of *Salmonella*: SopA(SipF), SopE, SopE2, and SipA(SspA) (Bronstein et al., 2000; Ehrbar et al., 2003, 2004; Lee and Galan, 2003). Therefore, a structural analysis of InvB in complex with one of its substrates has the potential to reveal commonalities in the nature of its binding interaction with four molecules.

Results

A Structural Domain in SipA that Overlaps the CBD

SipA, or *Salmonella* invasion protein A, contributes to cytoskeletal rearrangements by enhancing actin polymerization through its C-terminal domain (McGhie et al., 2001; Zhou et al., 1999). The C-terminal, actin binding domain of SipA spans residues 497–669 (Lilic et al., 2003), and the CBD of SipA has been shown to roughly correspond to residues 1–158 by yeast two-hybrid analysis (Bronstein et al., 2000). We found that it is possible to subdivide SipA into three regions: residues 48–264, which form a highly soluble, proteolytically stable
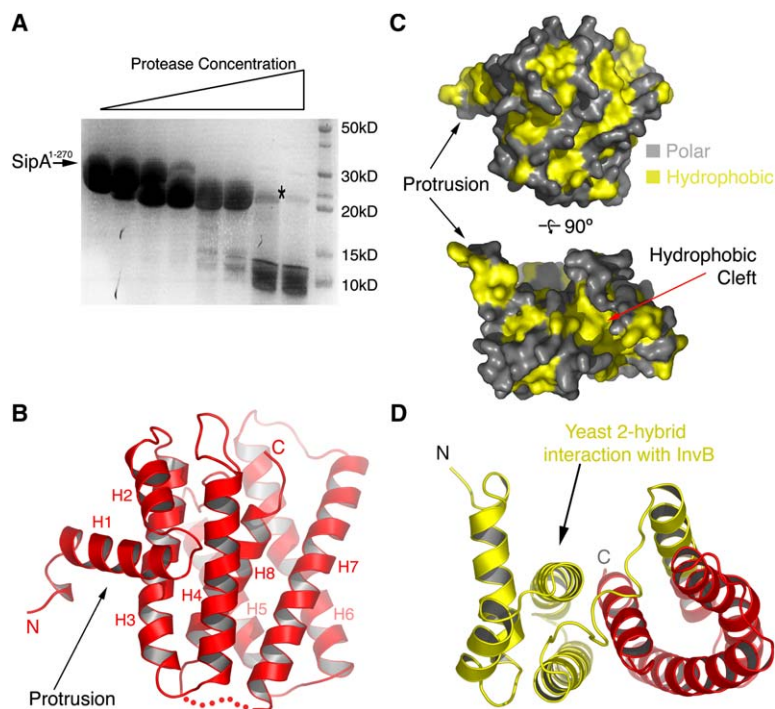
*Correspondence: stebbins@rockefeller.edu

A

C

B

D

Figure 1. An N-Terminal Structural Domain in *Salmonella* Invasion Protein A

(A) Proteolytic digestion of SipA$^{1-270}$ (Experimental Procedures). The asterisk indicates the band identified as SipA$^{48-264}$ by NH$_2$-terminal sequencing and mass spectroscopy.

(B) The overall fold of SipA$^{48-264}$ drawn as a ribbon diagram with secondary structure elements and NH$_2$-terminal protrusion labeled. Regions disordered in the crystal structure are shown as dotted lines connecting the appropriate regions of secondary structure. N, NH$_2$ terminus; C, COOH terminus.

(C) Molecular surface illustration of SipA$^{48-264}$ in two orientations in which hydrophobic regions are colored yellow and polar regions gray.

(D) A ribbon diagram of SipA$^{48-264}$ in which yellow highlights a portion of region (48–158) of the peptide identified by yeast two-hybrid analysis (1–158) as being sufficient in that assay to bind to the InvB chaperone.

domain (Figure 1A); a region spanning residues 270–400, which renders all constructs that contain it insoluble (data not shown); and the actin binding C-terminal domain, again a highly stable and soluble construct (Lilic et al., 2003).

The crystal structure of the N-terminal domain of SipA (residues 48–264, henceforth SipA$^{48-264}$) was determined by single anomalous diffraction from selenomethionine substituted protein and refined to 2.0 angstrom resolution (Experimental Procedures and Table 1). SipA$^{48-264}$ possesses an all-helical fold consisting of eight helices arranged so that six long, amphipathic helices form a compact fold that surrounds a final, predominantly hydrophobic helix in the middle of the molecule (Figure 1B, stereoimages in Figure S1, in the Supplemental Data available with this article online). Two N-terminal helices pack more loosely against this core fold, forming a small subdomain that extends into solution

Table 1. Crystallographic Data

	SipA(48–264) Native	SipA-InvB Native	SipA(48–264) SeMet	SipA-InvB SeMet
Data Collection				
Space group	P3$_2$21	P6$_5$22	P3$_2$21	P6$_5$22
Cell dimensions				
a, b, c (Å)	70.6, 70.6, 95.4	146.5, 146.5, 156.7	71.1, 71.1, 95.4	146.3, 146.3, 156.6
α, β, γ (°)	90, 90, 120	90, 90, 120	90, 90, 120	90, 90, 120
Wavelength	0.979	0.979	0.979	0.979
Resolution (Å)	99.0–2.0	99.0–2.2	50.0–2.8	50.0–2.4
R$_{sym}$	3.1 (35.7)	6.4 (59.2)	15.6 (42.2)	7.1 (57.9)
I/σI	38.3 (3.1)	29.3 (4.8)	22.3 (7.6)	29.3 (3.8)
Completeness (%)	99.0 (99.9)	99.3 (99.2)	99.5 (100.0)	100.0 (100.0)
Refinement				
Resolution (Å)	50.0–2.0	99.0–2.2		
No. reflections	18184	47001		
R$_{work}$/R$_{free}$	20.2/25.5	19.8/24.0		
No. atoms				
Protein	1633	3693		
Water	89	613		
Mean B factor	45.37	30.0		
Rms deviations				
Bond lengths (Å)	0.021	0.015		
Bond angles (°)	1.780	1.400		

R$_{sym}$ = $\sum h \sum i \mid I_{h,i} - I_h \mid / \sum h \sum i\, I_{h,i}$, for the intensity (*I*) of *i* observations of reflection *h*. Values in parentheses are for the high-resolution shell. R = $\sum \mid F$P − Fcalc $\mid / \sum F$P ; Fcalc = model structure factor and 5% data omitted for R$_{free}$. Bond and angle deviations are from ideal values.
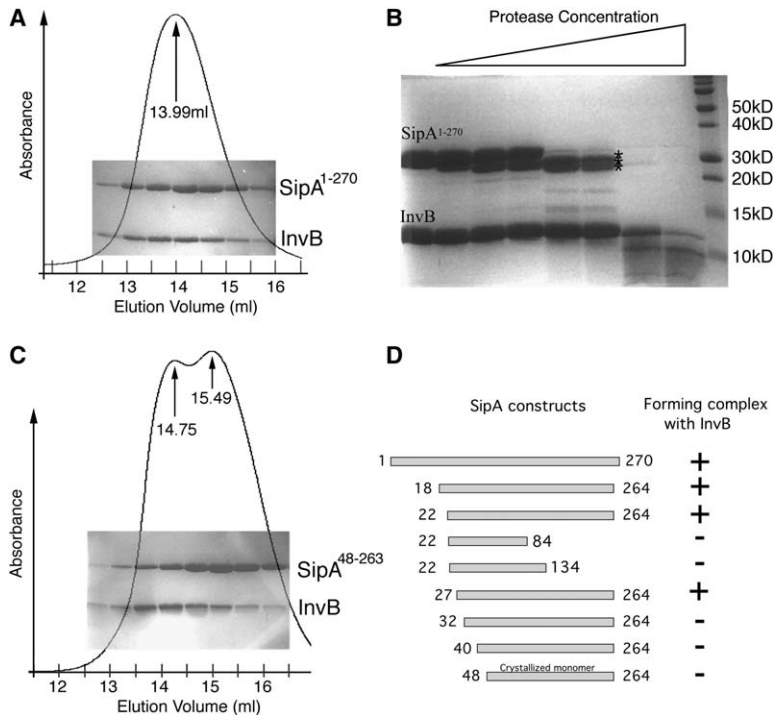
Figure 2. Delineation of the InvB Binding Domain of SipA

(A) Gel filtration chromatographic results (Experimental Procedures) showing stable complex formation between SipA(1–270) and InvB.

(B) Proteolytic digestion of the InvB-SipA(1–270) complex (see Experimental Procedures). The asterisk indicates those bands of SipA protected by InvB from digestion in which the NH$_2$ termini correspond to residues 44 and 48.

(C) Gel filtration chromatographic results (Experimental Procedures) showing that a stable complex does not form between SipA(48–264) and InvB.

(D) List of constructs of SipA and their ability to bind InvB as assayed by gel filtration chromatography.

(protrusion) with the last ten amino acids as a random coil that is characterized by partial disorder and high temperature factors (Figure 1B).

The molecular surface is characterized by several large hydrophobic patches that are mostly clustered to one side of the molecule, highlighting potential surfaces for protein-protein interactions (Figure 1C). In addition, the N-terminal protrusion is extensively hydrophobic, indicating a region very likely to be involved in binding other proteins.

Yeast two-hybrid analysis has shown that residues 1–158 are sufficient for an interaction with the chaperone InvB (Bronstein et al., 2000). Residues 48–158 correspond predominantly to one half of the structural domain, including the N-terminal protrusion, and the first five helices of the fold (Figure 1D). Should SipA bind its chaperone as a nonglobular polypeptide using this region, it would require a substantial unfolding of the observed structure. However, there are 47 amino acids N-terminal to this region that could serve as a nonglobular peptide for chaperone interaction. This region is proteolytically sensitive, perhaps indicating that it is unstructured in the absence of InvB (Figure 1A).

This structure raises several interesting questions. At the forefront is the seeming overlap of the InvB binding domain with a substantial portion of the stably folded SipA$^{48–264}$. We therefore turned to characterizing the InvB-SipA interaction, to ascertain if there was a nonglobular interaction as seen in all previous T3SS chaperone complexes, and, if so, whether this domain unfolded to provide the peptide for such an interaction.

Structure of a SipA-InvB Complex

SipA$^{1–270}$ can be expressed either independently of InvB or coexpressed with InvB in E. coli and in both cases forms a highly soluble and stable complex with its chaperone (Figure 2A). Limited proteolysis of the InvB-SipA$^{1–270}$ complex revealed that the chaperone and a stable subdomain identical with our SipA$^{48–264}$ complex were resistant to digestion (Figure 2B). However, SipA$^{48–264}$ was not able to form a stable complex with InvB, suggesting that residues N-terminal to 48 were necessary for a strong interaction (Figure 2C). A series of N-terminal deletions (Figure 2D) revealed that the first 21 amino acids were dispensable for InvB binding but that deletion beyond amino acid Leu27 significantly destabilized the SipA-InvB association. Fragments of SipA spanning residues 22–84 and 22–134 were also unable to bind to InvB. Surprisingly, these studies suggest that the integrity of the folded SipA$^{48–264}$ domain is required for stable InvB binding.

The crystal structure of the SipA(22–264)-InvB complex is remarkable for its similarities with, and important differences from, previous chaperone-virulence factor complexes in type III pathogenesis. The mode of interaction between SipA and InvB preserves the nonglobular character of the virulence factor CBD, but, intriguingly, this interaction occurs with only one of the InvB molecules in the chaperone homodimer (Figures 3A and 3B, stereoimages in Figures S1 and S2, and Table 1). This is in contrast to the interactions of Salmonella SptP with SicP, Yersinia YopE with SycE, and Yersinia YopN with the SycN/YscB heterodimeric chaperone, all of which involve a nonglobular polypeptide of the virulence factor that wraps around both molecules in the chaperone dimer. Central to those interactions is the use of the same hydrophobic surface patches on each chaperone to bind different regions of the nonglobular virulence factor peptide. For SipA, the nonglobular region instead interacts with the conserved hydrophobic patches of only one InvB molecule, leaving the other patches on the second InvB molecule exposed to solvent,
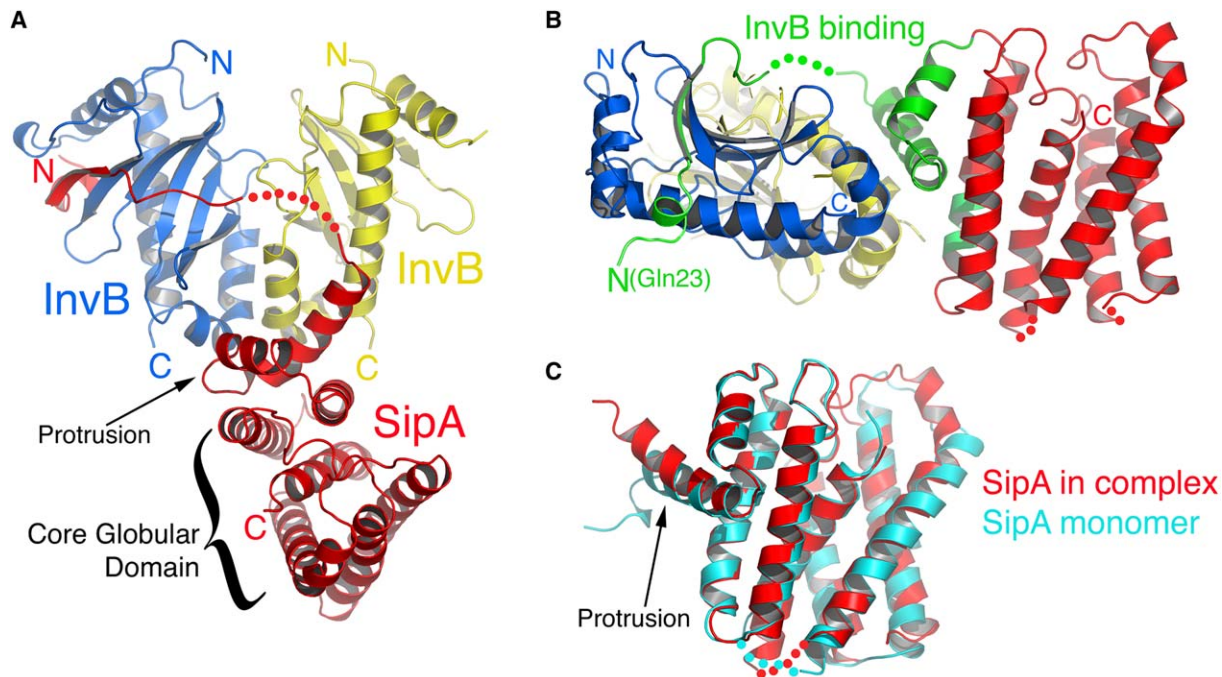
Figure 3. Crystal Structure of a SipA-InvB Complex

(A) Overall structure of the complex of InvB with SipA$^{22–264}$ depicted as a ribbon diagram. The two monomers of InvB are colored blue and yellow, whereas SipA is colored red. Regions disordered in the crystal structure are shown as dotted lines connecting the appropriate regions of secondary structure.

(B) A rotated view of (A) in which the InvB binding region of SipA is shown in green.

(C) Alignment of the globular domain of SipA from the SipA$^{48–264}$ structure and from the SipA-InvB complex.

contributing slightly more than one half (2300 Å^2) of the total 4000 Å^2 of surface area buried upon complex formation (Figures 4A–4C). For comparison, the complexes of SptP-SicP, YopE-SycE, and YopN with SycN-YscB bury approximately 6200 Å^2, 4600 Å^2, and 3600 Å^2, respectively.

The nonglobular contacts occur over hydrophobic tracks along the surface of one of the chaperones. Residues 45–51, which are disordered, are proximal to the second chaperone molecule (Figures 3A and 3B). Residues 36–47 extend over the "front" of the chaperone, and the side chains of Arg35, Glu36, and Ser43 make hydrogen bond contacts to InvB side chains Asp36, Ser29, Gln94, respectively (Figures 4A and 4C). Van der Waals contacts occur between InvB hydrophobic regions and SipA residue Leu42. In addition, a large number of side chain to main chain and main chain to main chain contacts occur over this stretch of SipA amino acids. The peptide then angles around the side of an InvB molecule, and residues 30–36 of SipA insert into a hydrophobic pocket forming an intermolecular β sheet with the chaperone, with residues Leu31 and Val34 binding in the pocket, whereas Asn30 and Arg35 make hydrogen bond contacts with InvB residues Tyr123 and Asp36, respectively (Figures 4A and 4C). Finally, the nonglobular domain begins with a short helix (residues 25–29) on the opposite face of the chaperone (Figure 4A), making both hydrophobic (Leu27 and Ala28) and hydrogen bond contacts (Thr25 to InvB Asn120).

The SipA$^{48–264}$ domain is not unfolded by the chaperone but interacts through its N-terminal, hydrophobic protrusion and through proximal helices via globular protein-protein contacts with both molecules of InvB. Roughly 30 amino acids from the N terminus are nonglobular, and residues 44–51, containing the site of protease cleavage (Figure 2B), are disordered. The remainder of the domain adopts a fold nearly identical to free SipA$^{48–264}$, aligning with a root-mean-square deviation in Cα positions of 1.1 Å (Figure 3C). The globular protein-protein interactions bury a respectable 1700 Å^2 of surface area and involve a more polar interface than that with the CBD (Figures 4B and 4C). Our binding analysis of deletion mutants (Figure 2D) and the large interface between the globular domain and InvB indicate that the nonglobular CBD of SipA is necessary, but not sufficient, for InvB association.

The observation that the nonglobular peptide of the SipA CBD did not bind the conserved hydrophobic patches on one of the InvB molecules suggested the possibility that the InvB homodimer could bind two effector molecules simultaneously. Simple modeling by aligning the chaperone and nonglobular peptide of SipA to the unbound InvB chaperone reveals that the globular domains clash severely, so that SipA is incapable of forming such a complex, consistent with our biochemical and crystallographic data. In addition, biochemical experiments show that with no combination of virulence factors can a stable ternary complex be formed (Figures S3A and S3B).

A Common Targeting Motif in Type III Secretion

When the known chaperone-substrate cocrystal structures are compared, the polypeptide chains of the substrates superimpose very closely at one region of the
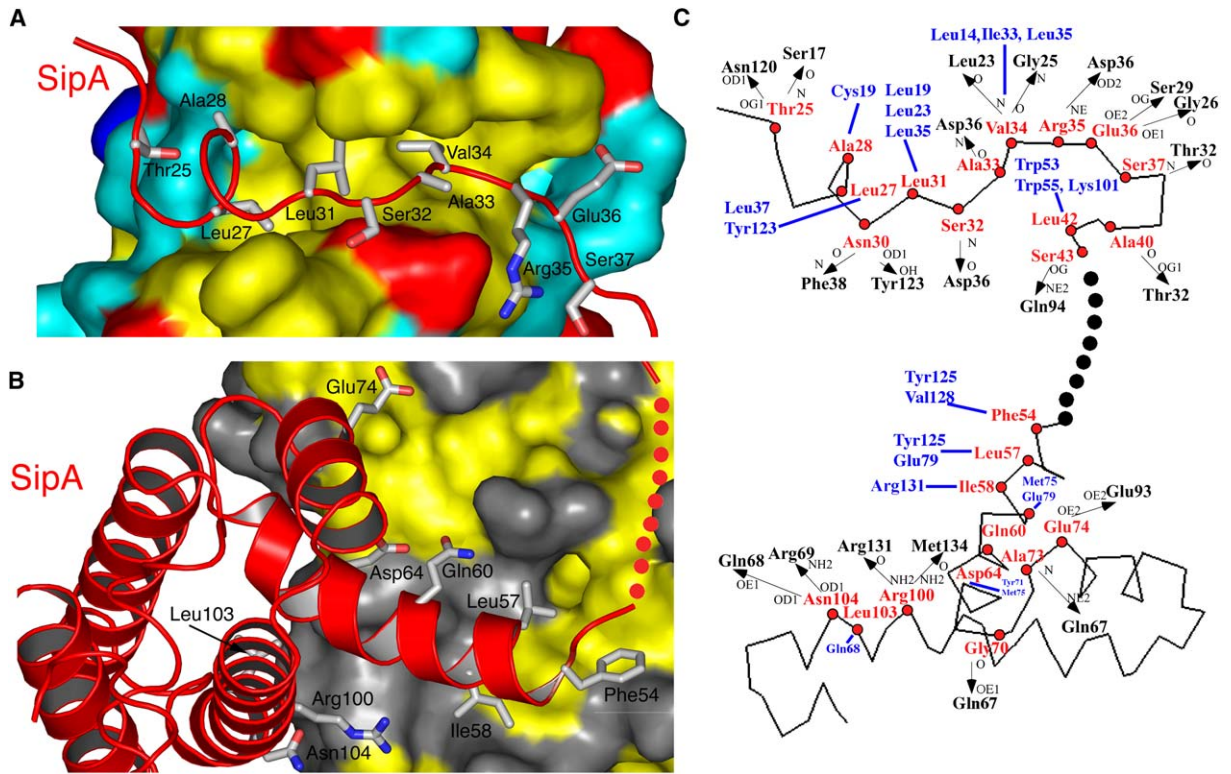
Figure 4. Globular and Nonglobular Interactions

(A) Nonglobular protein-protein interactions are shown with SipA drawn as a ribbon diagram with side chains and InvB depicted as a molecular surface colored such that hydrophobic residues are yellow, acidic residues are red, basic residues are blue, and all other polar residues are cyan.
(B) Globular interactions are shown with coloring as in (A), except that all polar residues in the chaperone are shown in gray. For clarity, some residues making contacts have been omitted (see [C]).
(C) Schematic of contacts between SipA and InvB. The SipA polypeptide chain is drawn with the Cα position of residues shown as a red sphere and the residues labeled in red. Van der Waals contacts to InvB residues are shown in blue and hydrogen bonds in black. The nonglobular domain is above the globular domain, and they are separated by the dashed line in black.

chaperone molecule (Figure 5A). At this region, the poly-peptide invariably forms an intermolecular β sheet with the chaperone, binding in a large hydrophobic crevice, into which it inserts several hydrophobic residues (Figures 5A and 5B). Although the remainder of the CBDs have related features in their interaction with other conserved hydrophobic patches, there is much more divergence in both the conformation of the backbone polypeptide as well as in the specifics of the interactions observed in these other regions (Figure 5A). Therefore, the formation of the intermolecular β sheet between chaperone and CBD and, in particular, the general similarities in the insertion of hydrophobic residues into this region prompted us to more closely examine this aspect of complex formation.

Beginning with SipA-InvB, there are three key residues making contacts in this region: Leu27, Leu31, and Val34, all of which insert into the hydrophobic patch of InvB (Figures 4A and 5B). When one compares the CBDs of the other InvB substrates—SopE, SopE2, and SopA—a striking pattern emerges (Figure 5D). Beginning with Leu27 near the start of the β strand, there is a high conservation of hydrophobic residues at positions 1, 5, and 8 (corresponding to Leu27, Leu31, and Val34 in SipA). These similarities strongly suggest that each of the substrates for InvB is targeted to this region of the chaperone by a similar motif.

This β strand motif is distributed much more broadly in T3SS substrates, however, which becomes clear upon extending this analysis beyond the InvB substrate family. A superposition of the β strand insertions from four known structures of CBDs bound to a T3SS chaperone reveals that, in three-dimensional space, the CBDs of YopE, SptP, YopN, and SipA possess very similar residues at these same positions (Figure 5C). Although at times the sequence positioning is different due to insertions or deletions, these alterations are absorbed in the tertiary structure, and the structural positioning is the same. The first two residues are always hydrophobic, whereas the third is very often hydrophobic with several exceptions (Figure 5D). However, in the known cocrystal structures, when the third residue is not hydrophobic, in many cases this residue contacts the chaperone in part through hydrophobic, van der Waals interactions. Therefore, the characterized chaperone-substrate interactions are each linked by a common binding motif.

Using this motif as a guide, we extended our analysis very broadly to a large set of virulence factor substrates of T3SS from diverse animal pathogens. To our surprise, this short β strand motif can be found in the N-terminal domains of a widespread group of virulence factors that are T3SS substrates (Figure 5D): peptides with this motif in the CBDs of translocated proteins can be identified in *Yersinia*, *Salmonella* (in both the SPI-1 and SPI-2
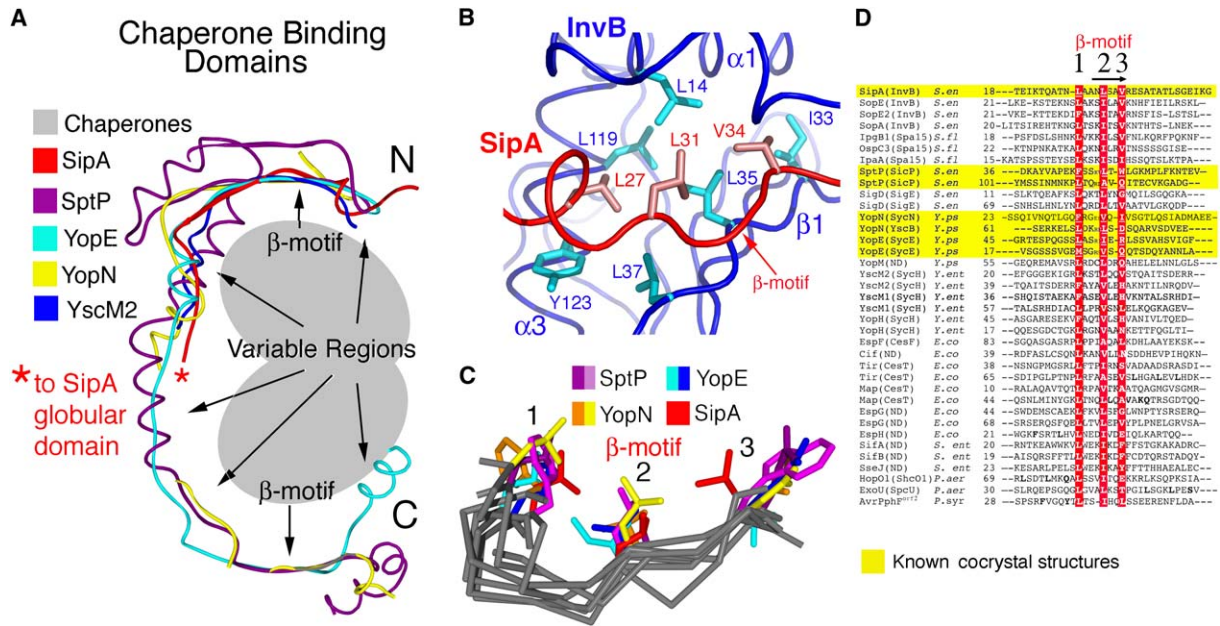
Figure 5. A Conserved Chaperone Binding Motif

(A) Superposition of the nonglobular polypeptides from the several cocrystal structures of T3SS chaperones and substrates. The β motif is indicated, as are the variable regions. In this illustration, the chaperone dimer would occupy the space on the inside of the virulence factor peptide path and is schematically shown in gray. "N" and "C" refer to the approximate termini of the CBDs. The asterisk indicates where in the CBD of SipA the polypeptide transitions from the nonglobular to the globular region.

(B) Illustration of the conserved interaction between a chaperone and the β motif, using SipA-InvB as an example. InvB is shown in blue for main chain, with the conserved pocket residues in cyan. SipA is shown with a red main chain and salmon side chain for the β motif. The chaperone secondary structural elements that present the interacting residues of the pocket are indicated.

(C) Superposition of the β motif from several cocrystal structures. The backbone polypeptide for each of the chains is shown in gray, whereas the side chains are colored as indicated. For those virulence factors that bind both chaperones in the dimer via distinct β motifs, dual colors are indicated. Numbers indicate the three conserved insertions into the chaperone hydrophobic pocket.

(D) Sequence alignment of T3SS substrate virulence factors from a multitude of animal and plant pathogens in which a β motif-like sequence could be identified. The motif residues are shown in white with a red background. A yellow background indicates those CBDs for which the cocrystal structure with the chaperone is available, and the contacts of the β motif in those cases are underlined.

pathogenicity islands), *Shigella*, *E. coli*, and *Pseudomonas*. Although several plant sequences appeared to harbor a similar motif, many did not, and it is likely that there is some divergence in the effector-chaperone interactions between animal and plant pathogens. The presence of the motif in several plant effectors suggests, however, that, in some cases, a similar interaction may occur.

A Conserved Binding Site in the Secretion Chaperones

Applying a "ligand-receptor" model to the T3SS substrate-chaperone interaction, it would be expected that the presence of the conserved β motif would necessitate a conserved binding feature in the chaperones. Ten structures currently exist of T3SS chaperones from animal and plant pathogens, and an analysis of their aligned structures does indeed reveal a highly conserved CBD interaction pocket. Six residues in the chaperones are conserved in character, three-dimensional location, and, significantly, in their propensity to bind to β motif residues (Figures 6A and 6B). Central to the interaction is the first β strand of the chaperone (β1) that forms an antiparallel, intermolecular β strand pairing with the β motif of the CBD (Figures 5B, 6A, and 6B). In this strand are three conserved hydrophobic residues oriented to face outwards and that interact with elements of the

β motif (e.g., Ile33, Leu35, and Leu37 of InvB, which interact with SipA Leu27, Leu31, and Val34, Figures 5B, 6A, and 6B). A highly conserved leucine (phenylalanine in SycN, Leu14 in InvB) extends from the "top" into the pocket from the first helix of the chaperone fold, and two C-terminal hydrophobic residues from the final α3 helix (Leu119 and Tyr123 of InvB) line the "bottom" of the pocket (Figures 5B, 6A, and 6B). There is some variation in these pocket residues, but the nonpolar nature predominates, and their three-dimensional positioning is conserved. Significantly, in the known complexes with CBDs, these residues are the only ones in this region to consistently make contacts with the β motif. Overall, the conserved β motif is matched by an equally well-conserved pocket in the chaperone molecules.

Examining the β Motif with Targeted Mutagenesis

We probed the biological significance of the β motif by examining deletion and directed point mutants in biochemical and bacterial secretion assays. Biochemically, deletions at the N terminus of SipA prior to the motif residues do not impair complex formation, whereas deletions of the motif destabilize the SipA-InvB complex (Figures 7A and 2D). A triple point mutant in which the three motif residues were altered (Leu27, Leu31, and Val34, all to glycine for a loss of contact phenotype, henceforth called SipAβ^{mut}) leads to an aggregation of
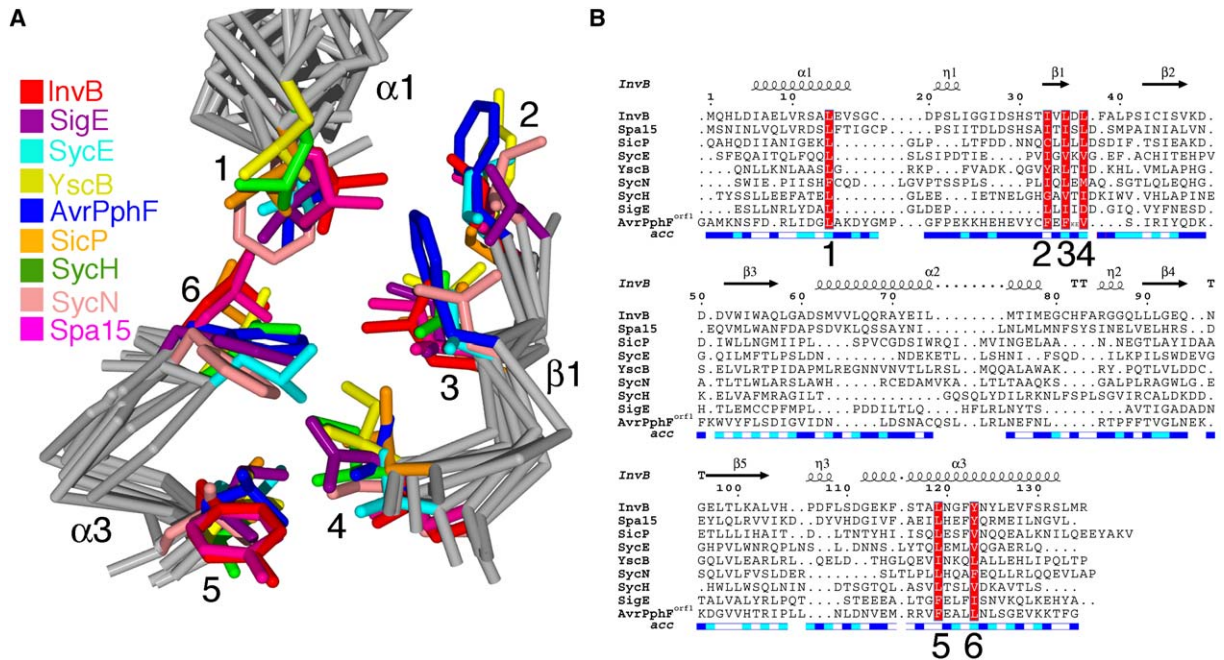
Figure 6. A Conserved Binding Pocket in Secretion Chaperones

(A) Structural alignment of several secretion chaperones, focusing on the conserved β motif binding pocket. The main chain is shown in gray, and the β motif binding residues, or residues that align structurally with those residues, are colored as indicated.

(B) Structure-based sequence alignment of nine T3SS chaperones. Residues in the hydrophobic pocket that contact β motif residues, and whose three-dimensional positioning is highly conserved, are shown in white with a red background. Secondary structure elements and the solvent accessibility for residues of InvB are shown (gradient from white, or buried, to dark blue, or exposed). Numbering is for InvB.

the complex as judged by gel filtration chromatography (Figure 7A). This aggregation is observed only when the mutant SipA is mixed with InvB: the SipAβ[mut] protein alone is a highly stable and soluble construct that is indistinguishable from wild-type SipA (Figure S4). Moreover, the deletion mutants behave likewise. As predicted from the structural data showing that this region plays no role in the folding of SipA, this indicates that these alterations have not destabilized SipA. They do, however, destabilize the SipA-InvB interaction. Therefore, the β motif appears to be critical to chaperone-substrate complex stability in vitro.

We also examined secretion through the SPI-1 T3SS of *Salmonella*, the physiological delivery system of SipA. Recent reports indicate that, in the absence of a chaperone interaction, some T3SS substrates, while not secreted through the pathogenic T3SS, can nonetheless be secreted (but not translocated into the host cell) through the evolutionarily related flagellar T3SS via an ancestral signal (Lee and Galan, 2004). We therefore looked at secretion of wild-type and mutant SipA in different strains of *Salmonella*, some of which were unable to assemble a functional flagellar T3SS (Experimental Procedures). The intracellular pools of the wild-type SipA and SipAβ[mut] are identical in *Salmonella*, indicating that the mutations have not destabilized the construct in vivo, consistent with the results of recombinant expression in *E. coli* and biochemical data discussed above (Figure 7B). Significantly, SipAβ[mut] was not secreted through the pathogenic T3SS (Figure 7B). In particular, similar to what was reported with the *Salmonella* effectors SptP and SopE in the absence of their CBDs (Lee and Galan, 2004), SipAβ[mut] was found secreted in wild-type *Salmonella* but not by a *fliGHI* null mutant strain of *Salmonella* that is defective in flagellar secretion (Lockman and Curtiss, 1990). This indicates that, without the β motif residues, SipA is no longer competent for secretion from the pathogenic T3SS but can still be engaged by the flagellar T3SS. In fact, merely by altering the three β motif residues in SipA, we can recapitulate the lack of secretion phenotype observed by wholescale deletion of the entire CBDs of SptP and SopE (Lee and Galan, 2004). Therefore, the biochemical and secretion data with the β motif mutants show that, for SipA, this chaperone binding motif is critical for the functioning of this pathogenic protein translocation system, conferring secretion pathway specificity (Lee and Galan, 2004).

To ascertain the generality of this result, we examined the effects of mutating the β motif in the *Salmonella* virulence factor SptP (with cognate chaperone SicP) as well as the virulence factors YopE and YopH from *Yersinia* spp (with chaperones SycE and SycH, respectively). SptP possesses two β motifs, each interacting with the same binding site in a different molecule in the chaperone homodimer (Figures 5A, 5C, and 5D). Mutation of the motif alone or both together leads to a nearly complete destabilization of the SptP-SicP complex as assayed by a pull-down experiment from bacterial coexpression (GST-SicP coexpressed with SptP), on ion-exchange chromatography, and by gel filtration chromatography (Supplemental Experimental Procedures and Figures S5A–S5F). Secretion assays mirror those of the β motif mutants for SipA: mutant SptP (a single β motif mutant) abolishes secretion from the pathogenic T3SS, although
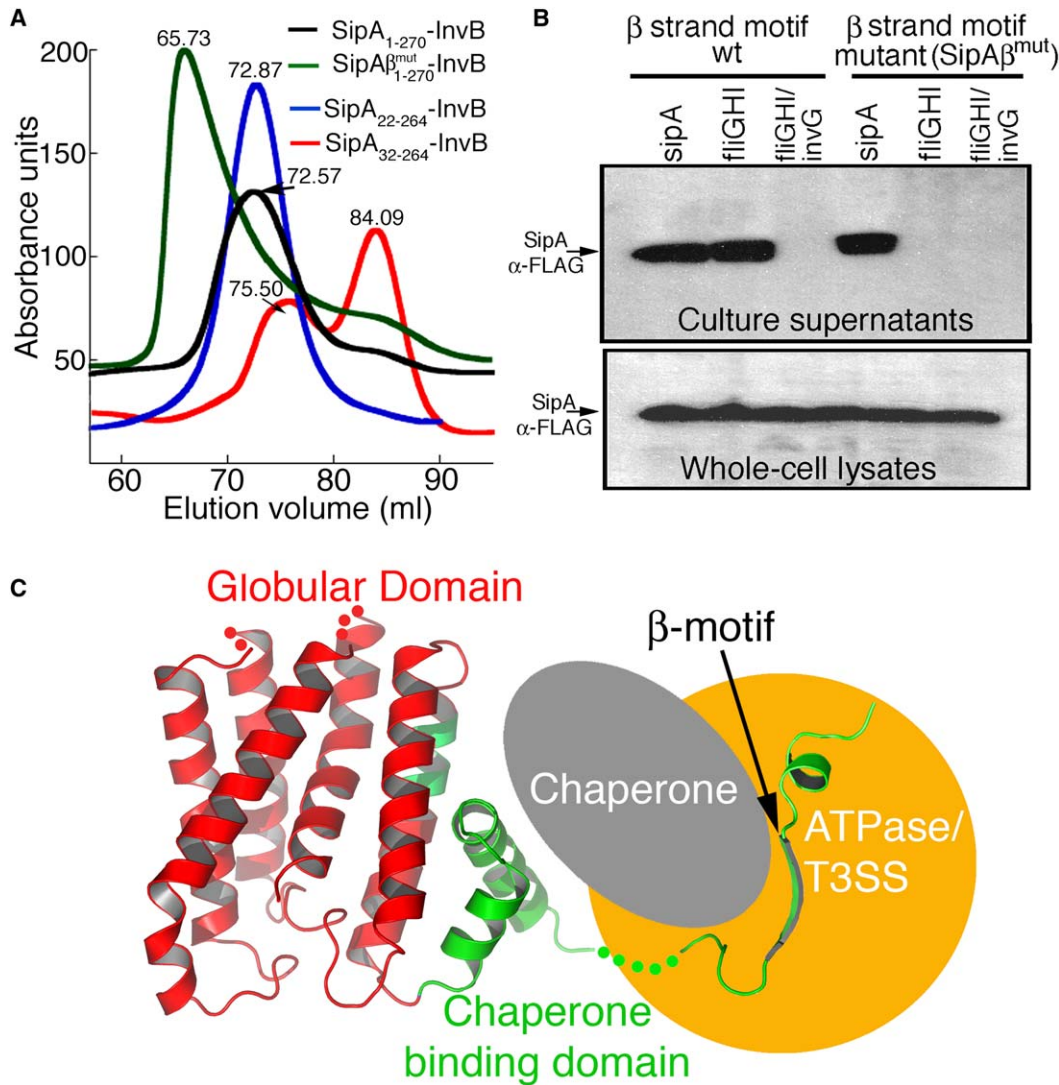
Figure 7. An Adaptor-Targeting Model Supported by the Biological Significance of the β Motif

(A) Deletion at the N terminus of SipA(32–264), encompassing the β strand motif, leads to destabilization of the SipA-InvB complex as assayed by gel filtration chromatography (red graph). The loss-of-contact triple (β strand motif) mutant, SipAβ^{mut}, causes an aggregation of a SipA-InvB mixture as judged by gel filtration chromatography (green graph). In contrast, stable complex formation at the appropriate molecular weight is observed with SipA(1–270) or SipA(22–264) with InvB (in black and blue, respectively). The elution volumes are indicated by numbers above the peaks.

(B) SipAβ^{mut} leads to a loss in secretion through the pathogenic T3SS of *Salmonella*. Culture supernatants and whole-cell lysates from several strains of *S. typhimurium* (Experimental Procedures) expressing SipA-FLAG and SipAβ^{mut}-FLAG were separated by SDS-PAGE and examined for the presence of the SipA protein by Western blot analysis. No secretion of SipAβ^{mut} is observed in a strain unable to assemble a functional flagellar T3SS (*fliGHI*), indicating that β motif is essential for secretion through the SPI-1 pathogenic T3SS.

(C) Model showcasing an adaptor-targeting system centered on the β motif illustrated using the globular and nonglobular domains of SipA. The ATPase and other elements of the T3SS are shown schematically in orange, the chaperones in gray, and SipA as a ribbon diagram from the crystal structure. Whether the β motif itself is recognized by the T3SS is unknown.

secretion can still occur through the flagellar system (Supplemental Experimental Procedures and Figure S6). Mutation of both β motifs in YopE leads to a loss of pulldown (GST-YopE coexpressed with SycE) and a lack of complex formation as assayed by anion exchange chromatography (Supplemental Experimental Procedures and Figures S7A–S7F). Complex formation by gel filtration chromatography is unaffected, indicating that the β motif mutations in YopE have, relative to SptP, less severely disrupted the interaction between chaperone and substrate. The effects with YopH are similar. The double mutant YopH β motif (as well as a single mutant in second putative β motif) leads to a disruption of the YopH-SycH complex by ion exchange but not gel filtration (Supplemental Experimental Procedures and Figures S8A–S8E). Therefore, these extensive binding interfaces (of several thousand square angstroms in all cases) can be disrupted by altering three or, at most, six residues. That this occurs for four T3SS substrates from two different pathogens argues, we believe, for the conserved importance of the β motif in chaperone-substrate interactions.

Discussion

T3SSs are central to the virulence of a diverse range of animal and plant pathogens. The binding of virulence factor substrates to specialized chaperones in the bacteria is critical to the functioning of these systems. Using the InvB chaperone of *Salmonella*, we have identified through a sequence and structural analysis of many different T3SS substrates and chaperones a common receptor-ligand type of interaction, involving a common binding motif present in a short peptide of the virulence factors and a conserved hydrophobic pocket in the chaperones.

The relative contribution to binding affinity of this motif for a given chaperone-substrate complex is likely to vary, as additional binding elements may contribute significantly to chaperone-substrate interactions. For example, a single β motif mutation in SptP was sufficient to prevent complex formation and secretion, whereas it required both β motifs to be altered in YopE to achieve complex disruption. In addition, the accurate identification of the β motif by sequence bioinformatics may prove challenging in many cases. As we show in Figure 5D, the amino acids in the β motif that make interactions with their chaperone molecules (as verified by cocrystal structures) are variable both in residue nature and sequence positioning (due to one or two amino acid insertions and deletions). This is due to the rather "forgiving" nature of the β motif binding pocket in the chaperones. For substrates with two β motifs that interact with each pocket in the two chaperones of the homodimer, one can observe the same chaperone pocket to bind completely different sequences. For example, in YopE, the corresponding pocket insertion residues are M, V, and Q and L, I, and R for the two β motifs. In SptP, they are L, A, and Q and F, L, and W. Thus, even in the same chaperone, the sequence can vary for the β motif binding in the pocket.

The five cocrystal structures of CBDs with their chaperones reveal that there is significantly more variation in these interactions than was initially appreciated, and the β motif is the only conserved element present in all of these complexes. Therefore, it is unlikely that the overall three-dimensional paths of the CBDs could serve as a conserved signal to the T3SS, as has been proposed (Birtalan et al., 2002). Overall, the polypeptide paths are too different for such a conserved function.

One possibility, however, is that other aspects of the CBDs could target the bound virulence factor to the secretion apparatus alone or together with the chaperone. The strand harboring the β motif is an obvious candidate for a CBD-based signal to the secretion apparatus, but there is not so clear a pattern as the β motif, and, without the knowledge of the binding interaction to the T3SS, it is hard to test this hypothesis at present. Due to the importance of the β motif, at least in the cases of the four substrates examined, mutation of residues in this region, even those that do not contact the chaperone, may exert an effect on chaperone binding. In that case, it would be difficult to distinguish between a destabilization of the CBD-chaperone interaction that prevents appropriate secretion and a case in which such a putative signal was disrupted. Finally, since recent data show that T3SS chaperones alone are sufficient to bind to the highly conserved ATPase associated with the secretion apparatus (Gauthier and Finlay, 2003; Akeda and Galan, 2005), it is probable that an unappreciated common surface feature of the chaperones serves a targeting role independently of the CBD.

For these reasons, we favor an "adaptor-targeting" model for the delivery of secretion substrates to the pathogenic T3SS (Figure 7C). In this model, the β motif of the CBD plays the role of a conserved adaptor element that targets the virulence substrate to the chaperone. The chaperone alone, or in concert with the far N-terminal signal peptide and other potential signals in the CBD, then acts as a secondary adaptor that docks the substrate to the secretion apparatus. Such a system would convey an informational signal that distinguishes the T3SS substrates from all other proteins in the bacterium but also provides many avenues for the regulation of virulence factor delivery.

Such an adaptor model for T3SS is also consistent with other proposed roles of the chaperones, such as that of maintaining effectors in a secretion competent state (Stebbins and Galan, 2001a, 2003). This proposed function hypothesizes that the highly uncommon protein-protein interaction involving an extended nonglobular polypeptide in the CBD may "prime" the secretion substrate by presenting to the apparatus an extended segment of polypeptide in the nonglobular conformation required for traversal through the secretion system. The associated ATPase upon engagement with the nonglobular peptide would, in an energy-dependent fashion, actively pull the peptide through and unfold the remainder of the protein. This model does not suggest that priming is necessary for secretion, only that it would make it more efficient, or, in the case of a regulator that could recognize the CBD, perhaps serve as a point of negative or positive regulation. As it was initially proposed and elaborated (Stebbins and Galan, 2001a, 2003), this model also does not postulate any "unfolding" activity on the part of the chaperone to the remainder of the virulence factor, nor, in fact, to the CBD domain itself—activities clearly unlikely in such a small protein devoid of ATPase activity. It instead serves as a platform on which the nonglobular polypeptide of the CBD can "fold" and yet be maintained in a productive nonglobular conformation.

The β motif may constitute an important component of an ancient signal for pathogenic type III secretion, a motif still largely present in most T3SS substrates despite the enormous divergence in these bacteria and gene mixing from horizontal acquisition of virulence factors. This perspective may allow for a greater conceptual unity in this important virulence system and should prove useful for probing virulence factor delivery and chaperone binding as well as providing a target for pharmacological disruption of this conserved interaction.

Experimental Procedures

Protein Purification, Domain Delineation, and Complex Formation

SipA$^{1-270}$ was cloned as an NH$_2$-terminal glutathione S-transferase (GST) fusion, expressed in *E. coli* strain BL21 (DE3) by induction with 1 mM IPTG for 16 hr at 20°C, affinity purified on a glutathione-Sepharose resin (Amersham), and cleaved from GST by site specific proteolysis. SipA$^{1-270}$ was separated from GST on a Q-Sepharose

resin (Amersham) and further purified by gel filtration chromatography. The purified protein (4 μg per reaction) was then subjected to limited proteolysis with subtilisin for 30 min at 20°C. A stable fragment was identified through N-terminal sequencing and mass spectroscopy as SipA[48–264], which was subcloned and purified following the same procedure for SipA[1–270]. Selenomethionine-substituted SipA[48–264] protein was prepared by standard protocols (Doublie, 1997) and purified as SipA[48–264]. For the formation of the SipA-InvB complex, InvB was cloned by PCR from *Salmonella* SL1344 genomic DNA with an NH_2-terminal hexahistidine tag and expressed in *E. coli* strain BL21 (DE3) at 20°C by induction with 1 mM IPTG. InvB was affinity purified on a Ni-NTA agarose resin (Qiagen), and complex formation with different SipA constructs was tested by mixing and incubation for 2 hr at +4°C. The preparation and expression of SipA constructs used for analyzing complex formation with InvB was the same as above, with the exceptions of SipA[22–84] and SipA[22–134] that, due to insolubility, were purified under denaturing conditions (8 M urea, 10 mM Tris [pH 8.0], 0.1 M sodium phosphate). In this case, SipA proteins were subsequently mixed with denatured InvB (as a control, the refolding with SipA[1–270] and SipA[48–264] yield a soluble and stable complex). Protein complex formation was assayed by gel filtration chromatography (Superdex 200 from Amersham equilibrated in 25 mM Tris [pH 8.0], 200 mM NaCl, and 2 mM dithiothreitol, or DTT). For crystallization, SipA[22–264]-InvB was subjected to reductive methylation (Rypniewski et al., 1993) followed by a final step of gel filtration chromatography. Selenomethionine-substituted SipA[22–264] was purified and used for complex formation with InvB, and this protein complex was also subjected to reductive methylation. The methods for other InvB substrates, as well as SptP, YopH, and YopE, are described in the Supplemental Experimental Procedures.

Structural Determination

For crystallization, the purified preparation of SipA[48–264] was concentrated to 20 mg/ml in a buffer containing 25 mM Tris (pH 8.0), 200 mM NaCl, and 2 mM DTT. Crystals of the SipA[48–264] were grown by vapor diffusion using hanging drops formed from mixing a 1:1 volume ratio of 20 mg/ml protein with an equilibration buffer consisting of 20% PEG6000, 20% glycerol, Na citrate (pH 5.6), and 0.01 M adenosine-5′-triphosphate disodium salt (ATP) as an additive. For cryoprotection, crystals were transferred into 25% glycerol and frozen immediately in a stream of gaseous nitrogen (−170°C).

For crystallization of the SipA[22–264]-InvB complex, the reductively methylated protein complex was concentrated to 27 mg/ml in a buffer containing 25 mM Tris (pH 8.0), 200 mM NaCl, and 2 mM DTT. Crystals of the protein complex were grown at room temperature by vapor diffusion using hanging drops formed from mixing a 1:1 volume ratio of 27 mg/ml protein with an equilibration buffer consisting of 3.8 M Na formate, 0.9 M Na cacodylate (pH 5.2), and 0.09 M guanidine-hydrochloride as an additive. For cryoprotection, crystals were transferred into 6 M Na formate and frozen immediately in a stream of gaseous nitrogen (−170°C). For both SipA[48–264] and the SipA[22–264]-InvB complex, data were collected at Brookhaven National Synchrotron Light Source beamline X9A at the peak energy to maximize the anomalous signal for selenium. Data were processed using the HKL software package (Otwinowski and Minor, 1997).

The positions of the selenium atoms for both SipA[48–264] and the SipA[22–264]-InvB complex, as well as the initial phases, were determined using the SHELXD and SHELXE (Schneider and Sheldrick, 2002), respectively, using the anomalous signal. The SHELXE phases were used in ARP/wARP (Perrakis et al., 1999) to create largely complete models and those models used with ARP/wARP to build and refine against native data. The model generated by ARP/wARP was then refined using REFMAC5 (Murshudov et al., 1997) from the CCP4 suite of programs. Both restrained refinement and refinement by TLS (Winn et al., 2001, 2003) were used. Several cycles of model building with O and refinement with REFMAC5 produced the final models with an R/R_{free} of 20.2%/25.5% and 19.6%/23.9% for SipA[48–264] and the SipA[22–264]-InvB complex, respectively. The models possess good stereochemistry, with 97.2% and 95.3% of the residues in the most favored regions of the Ramchandran plot for SipA[48–264] and the SipA[22–264]-InvB complex, respectively. Difference density at three solvent-exposed cysteine residues (InvB Cys44, and SipA Cys197 and Cys225) shows a large, nearly spherical

region around the sulfur atom. This we believe to be an artifact of the methylation reaction, although this was not examined by chemical analysis. The density was not modeled in the deposited coordinate file. Cysteines buried from solvent did not have this additional density. Helix H6 of SipA undergoes a conformational change between the monomer and chaperone complex crystals. This change consists of a translation by one turn of the helix, leaving the hydrophobic residues that pack in the core still appropriately oriented. This shift occurs with a complete reordering of the loop preceding H6, and selenomethionine sites for Met 224 aid in confirming this conformational alteration. It is unclear what has triggered this conformational change, although the presence of Cys225, with its methylation-induced covalent modification, may have contributed.

Mutagenesis

The loss-of-contact triple mutant of SipA(1–270), altering the β motif residues (denoted SipAβ[mut]), was made by in vitro site-directed mutagenesis using oligonucleotide primer pairs containing the mutations Leu27Gly, Leu31Gly, and Val34Gly. The amplification of the mutant plasmid was performed by Pfu Turbo DNA polymerase (Stratagene) in the thermal temperature cycler, and wild-type template plasmid was removed by digestion with DpnI before transformation. The introduced mutations were verified by DNA sequencing. The deletion mutant SipA(32–264) was generated by PCR and cloned into the same vector as previously described for SipA(1–270). SipAβ[mut] and all deletion mutants were expressed in *E. coli* strain BL21 (DE3), and purification of the mutant proteins and testing of their interaction with InvB was performed as previously described for the wild-type SipA protein. Mutants in SptP, YopE, and YopH are described in the Supplemental Experimental Procedures.

Bacterial Secretion Assay

Bacterial secretion assays were performed with wild-type SipA(1–270) and SipAβ[mut] with a C-terminal fusion of FLAG epitope (Asp-Tyr-Lys-Asp-Asp-Asp-Asp-Lys). These constructs were cloned into the low copy number vector pWKS30 (Wang and Kushner, 1991) and expressed under the control of the native promoter. Plasmids were introduced into a *sipA* mutant strain of *Salmonella* (SB225), a *fliGHI* mutant strain of *Salmonella* (SB181), and *fliGHI/invG* double mutant strain of *Salmonella* (SB763) by electroporation (Kaniga et al., 1995; Lockman and Curtiss, 1990).

Salmonella strains harboring wild-type SipA-FLAG or SipAβ[mut]-FLAG were grown in L broth supplemented with 0.3 M NaCl under the conditions that stimulate the expression of the SPI-1 T3SS. Bacterial secretion assays were performed as previously reported (Lee and Galan, 2004). Briefly, whole cells and culture supernatants were separated by centrifugation, and whole cells (0.2 ml) were resuspended in SDS-PAGE loading buffer. Culture supernatants (10 ml) were passed through a 0.4 μm filter and precipitated in the presence of 10% trichloroacetic acid (TCA) for 2 hr at 4°C. Precipitated culture supernatant pellets were washed with acetone, centrifuged, and resuspended in SDS-PAGE loading buffer. Whole-cell lysate and culture supernatant samples were separated on 15% SDS-PAGE, transferred on nitrocellulose membrane, and examined by Western blot analysis performed using a chemoluminescence detection system (GE Healthcare). Wild-type SipA and SipAβ[mut] were detected with monoclonal antibodies directed to the FLAG epitope (Sigma-Aldrich). The bacterial secretion assay of SptP wild-type and the β mutant protein was performed similarly (see Supplemental Experimental Procedures).

Supplemental Data

Supplemental Data include Supplemental Experimental Procedures and eight figures and can be found with this article online at http://www.molecule.org/cgi/content/full/21/5/653/DC1/.

Acknowledgments

References

Akeda, Y., and Galan, J.E. (2005). Chaperone release and unfolding of substrates in type III secretion. Nature *437*, 911–915.

Barbieri, J.T., Riese, M.J., and Aktories, K. (2002). Bacterial toxins that modify the actin cytoskeleton. Annu. Rev. Cell Dev. Biol. *18*, 315–344.

Birtalan, S.C., Phillips, R.M., and Ghosh, P. (2002). Three-dimensional secretion signals in chaperone-effector complexes of bacterial pathogens. Mol. Cell *9*, 971–980.

Bronstein, P.A., Miao, E.A., and Miller, S.I. (2000). InvB is a type III secretion chaperone specific for SspA. J. Bacteriol. *182*, 6638–6644.

Cornelis, G.R. (2000). Type III secretion: a bacterial device for close combat with cells of their eukaryotic host. Philos. Trans. R. Soc. Lond. B Biol. Sci. *355*, 681–693.

Doublie, S. (1997). Preparation of selenomethionyl proteins for phase determination. Methods Enzymol. *276*, 523–530.

Ehrbar, K., Friebel, A., Miller, S.I., and Hardt, W.D. (2003). Role of the *Salmonella* pathogenicity island 1 (SPI-1) protein InvB in type III secretion of SopE and SopE2, two *Salmonella* effector proteins encoded outside of SPI-1. J. Bacteriol. *185*, 6950–6967.

Ehrbar, K., Hapfelmeier, S., Stecher, B., and Hardt, W.D. (2004). InvB is required for type III-dependent secretion of SopA in *Salmonella* enterica serovar Typhimurium. J. Bacteriol. *186*, 1215–1219.

Galan, J.E. (2001). *Salmonella* interactions with host cells: type III secretion at work. Annu. Rev. Cell Dev. Biol. *17*, 53–86.

Galan, J.E., and Collmer, A. (1999). Type III secretion machines: bacterial devices for protein delivery into host cells. Science *284*, 1322–1328.

Gauthier, A., and Finlay, B.B. (2003). Translocated intimin receptor and its chaperone interact with ATPase of the type III secretion apparatus of enteropathogenic *Escherichia coli*. J. Bacteriol. *185*, 6747–6755.

Ghosh, P. (2004). Process of protein transport by the type III secretion system. Microbiol. Mol. Biol. Rev. *68*, 771–795.

Hueck, C.J. (1998). Type III protein secretion systems in bacterial pathogens of animals and plants. Microbiol. Mol. Biol. Rev. *62*, 379–433.

Kaniga, K., Trollinger, D., and Galan, J.E. (1995). Identification of two targets of the type III protein secretion system encoded by the inv and spa loci of *Salmonella typhimurium* that have homology to the Shigella IpaD and IpaA proteins. J. Bacteriol. *177*, 7078–7085.

Lee, S.H., and Galan, J.E. (2003). InvB is a type III secretion-associated chaperone for the *Salmonella enterica* effector protein SopE. J. Bacteriol. *185*, 7279–7284.

Lee, S.H., and Galan, J.E. (2004). *Salmonella* type III secretion-associated chaperones confer secretion-pathway specificity. Mol. Microbiol. *51*, 483–495.

Lerm, M., Schmidt, G., and Aktories, K. (2000). Bacterial protein toxins targeting rho GTPases. FEMS Microbiol. Lett. *188*, 1–6.

Lilic, M., Galkin, V.E., Orlova, A., VanLoock, M.S., Egelman, E.H., and Stebbins, C.E. (2003). *Salmonella* SipA polymerizes actin by stapling filaments with nonglobular protein arms. Science *301*, 1918–1921.

Lockman, H.A., and Curtiss, R., III. (1990). *Salmonella typhimurium* mutants lacking flagella or motility remain virulent in BALB/c mice. Infect. Immun. *58*, 137–143.

Luo, Y., Bertero, M.G., Frey, E.A., Pfuetzner, R.A., Wenk, M.R., Creagh, L., Marcus, S.L., Lim, D., Sicheri, F., Kay, C., et al. (2001). Structural and biochemical characterization of the type III secretion chaperones CesT and SigE. Nat. Struct. Biol. *8*, 1006–1008.

McGhie, E.J., Hayward, R.D., and Koronakis, V. (2001). Cooperation between actin-binding proteins of invasive *Salmonella*: SipA potentiates SipC nucleation and bundling of actin. EMBO J. *20*, 2131–2139.

Murshudov, G.N., Vagin, A.A., and Dodson, E.J. (1997). Refinement of macromolecular structures by the maximum-likelihood method. Acta Crystallogr. D Biol. Crystallogr. *53*, 240–255.

Otwinowski, Z., and Minor, W. (1997). Processing of X-ray diffraction data collected in oscillation mode. Methods Enzymol. *276*, 307–326.

Parsot, C., Hamiaux, C., and Page, A.L. (2003). The various and varying roles of specific chaperones in type III secretion systems. Curr. Opin. Microbiol. *6*, 7–14.

Perrakis, A., Morris, R., and Lamzin, V.S. (1999). Automated protein model building combined with iterative structure refinement. Nat. Struct. Biol. *6*, 458–463.

Phan, J., Tropea, J.E., and Waugh, D.S. (2004). Structure of the *Yersinia pestis* type III secretion chaperone SycH in complex with a stable fragment of YscM2. Acta Crystallogr. D Biol. Crystallogr. *60*, 1591–1599.

Ramamurthi, K.S., and Schneewind, O. (2003). Substrate recognition by the *Yersinia* type III protein secretion machinery. Mol. Microbiol. *50*, 1095–1102.

Rypniewski, W.R., Holden, H.M., and Rayment, I. (1993). Structural consequences of reductive methylation of lysine residues in hen egg white lysozyme: an X-ray analysis at 1.8 Å resolution. Biochemistry *32*, 9851–9858.

Schiavo, G., and van der Goot, F.G. (2001). The bacterial toxin toolkit. Nat. Rev. Mol. Cell Biol. *2*, 530–537.

Schneider, T.R., and Sheldrick, G.M. (2002). Substructure solution with SHELXD. Acta Crystallogr. D Biol. Crystallogr. *58*, 1772–1779.

Schubot, F.D., Jackson, M.W., Penrose, K.J., Cherry, S., Tropea, J.E., Plano, G.V., and Waugh, D.S. (2005). Three-dimensional structure of a macromolecular assembly that regulates type III secretion in *Yersinia pestis*. J. Mol. Biol. *346*, 1147–1161.

Singer, A.U., Desveaux, D., Betts, L., Chang, J.H., Nimchuk, Z., Grant, S.R., Dangl, J.L., and Sondek, J. (2004). Crystal structures of the type III effector protein AvrPphF and its chaperone reveal residues required for plant pathogenesis. Structure (Camb.) *12*, 1669–1681.

Stebbins, C.E., and Galan, J.E. (2001a). Maintenance of an unfolded polypeptide by a cognate chaperone in bacterial type III secretion. Nature *414*, 77–81.

Stebbins, C.E., and Galan, J.E. (2001b). Structural mimicry in bacterial virulence. Nature *412*, 701–705.

Stebbins, C.E., and Galan, J.E. (2003). Priming virulence factors for delivery into the host. Nat. Rev. Mol. Cell Biol. *4*, 738–743.

van Eerde, A., Hamiaux, C., Perez, J., Parsot, C., and Dijkstra, B.W. (2004). Structure of Spa15, a type III secretion chaperone from *Shigella flexneri* with broad specificity. EMBO Rep. *5*, 477–483.

Wang, R.F., and Kushner, S.R. (1991). Construction of versatile low-copy-number vectors for cloning, sequencing and gene expression in *Escherichia coli*. Gene *100*, 195–199.

Wattiau, P., Woestyn, S., and Cornelis, G.R. (1996). Customized secretion chaperones in pathogenic bacteria. Mol. Microbiol. *20*, 255–262.

Winn, M.D., Isupov, M.N., and Murshudov, G.N. (2001). Use of TLS parameters to model anisotropic displacements in macromolecular refinement. Acta Crystallogr. D Biol. Crystallogr. *57*, 122–133.

Winn, M.D., Murshudov, G.N., and Papiz, M.Z. (2003). Macromolecular TLS refinement in REFMAC at moderate resolutions. Methods Enzymol. *374*, 300–321.

Zaharik, M.L., Gruenheid, S., Perrin, A.J., and Finlay, B.B. (2002). Delivery of dangerous goods: type III secretion in enteric pathogens. Int. J. Med. Microbiol. *291*, 593–603.

Zhou, D., Mooseker, M.S., and Galan, J.E. (1999). Role of the *S. typhimurium* actin-binding protein SipA in bacterial internalization. Science *283*, 2092–2095.

Accession Numbers

Coordinates for the SipA$^{48-264}$ and the SipA$^{22-264}$-InvB complex have been deposited into the Protein Data Bank with ID codes 2FM9 and 2FM8, respectively.